

PACS numbers: 42.62.Fi, 78.47.+p, 78.20.-e, 78.20.Bh
DOI: 10.1070/QE2002v032n09ABEH002292

Degenerate four-wave mixing spectroscopy of ultrathin Au and Pt films

Yu.V. Bobyrev, V.M. Petnikova, K.V. Rudenko, V.V. Shuvalov

***Abstract*. The results of experimental investigations of ultrathin (30 – 40 nm) metal Au and Pt films by means of picosecond degenerate four-wave mixing spectroscopy are presented. Within the model of nonlinear response formation, which takes into account the coherent superposition of contributions from many saturable interband transitions in the real spectrum of electronic states, the characteristic intraband relaxation times are determined to be 230 ± 30 fs and 180 ± 30 fs for Au and Pt films, respectively. The temperature of the electron subsystem is found to be 600 – 800 K.**

Keywords: *four-wave mixing spectroscopy, ultrathin films, electronic spectra.*

1. Introduction

In recent years, much interest has been focused on the investigations of the ultrafast relaxation kinetics of 'impact' electron excitation in metals, which is usually realised by using ultrafast optical (laser) pulses [1 – 6]. In these studies, nonequilibrium states have been described by statistical parameters (the temperature T_e of the electron subsystem, the temperature T_p of the phonon subsystem, the position E_F of the Fermi level, etc.). These parameters are inaccessible to direct measurements and have been evaluated only indirectly. The method of picosecond degenerate four-wave mixing (DFWM) spectroscopy [7, 8], based on the probing of the space-modulated distribution of the dielectric constant 'written' in the tested sample (the Bragg grating), can be used in such investigations.

The grating is written when the tested sample is exposed to an interference field (with a spatially inhomogeneous distribution of the intensity I) of two picosecond pump pulses with the same carrier frequency propagating at some angle to one another. The grating is probed (i.e., the efficiency η of diffraction of one of the pump pulses from the grating in the process of self-diffraction is measured as a function of the wavelength λ) simultaneously with writing. Note that the method of DFWM spectroscopy is usually employed to obtain the information on resonance mechanisms of nonlinearity, i.e., to identify and qualitatively determine the spectral positions and the widths of resonances observed in the total nonlinear response, as well as the ratio of their amplitudes [7].

Even the first DFWM investigations of ultrathin Ni and Au films showed that η is highly sensitive to λ [8]. Based on the analysis of their data, the authors of [9] assumed that the processes of saturation of interband electronic transitions play the key role in the formation of the nonlinear response of metals at least within the visible range. These authors have also proposed a model of the electronic part of the nonlinear response $\eta(\lambda)$, which included the contributions from all possible one- and two-photon interband electronic transitions in the real energy-band structure of the sample under study.

It was found that the results of numerical simulation for ultrathin Ni films almost precisely followed the experimental data for intraband relaxation times $T_2 = 200 - 250$ fs. The major role of interband transitions in the formation of the transient response of several metal films (Ni, Au, and Cu) to an ultrafast optical pulse was pointed out by the authors of [10 – 12], who interpreted the data of experiments performed for different modifications of the pump-probe method.

Note that taking into account excess (light-induced) free carriers radically changes conventional concepts of the thermal mechanism of energy exchange between excited electron and phonon subsystems in metals [13]. Removal of the prohibition on the inelastic scattering of carriers at the surface [14], opens a fast relaxation channel for electron excitation energy [15]. Due to this channel, up to 10 % of absorbed energy can be transferred into the energy of surface deformation in a metal film with the thickness $L = 20$ nm during the time of the pulse $\tau_p = 20$ ps [16].

In this paper, we present and interpret the results of experiments performed with ultrathin ($L \approx 30 - 40$ nm) Au and Pt metal films by means of picosecond DFWM spectroscopy.

2. Experimental

In our experiments, we employed a pulsed (the pulse repetition rate is 1 – 5 Hz) passively mode-locked (dye No. 3274u in a polymer matrix, the mode-locking probability is ~ 98 %) picosecond Nd^{3+} : YAG master oscillator (MO). The linearly polarised radiation of the MO (a train of pulses with a duration of ~ 40 ps and an energy of ~ 2 mJ) was frequency-doubled in a KDP crystal (40-mm long, oe – e interaction) with an efficiency of ~ 30 %. A system of mirrors and focusing lenses coupled this radiation into

Yu.V. Bobyrev, V.M. Petnikova, K.V. Rudenko, V.V. Shuvalov International Teaching and Research Laser Center, M.V. Lomonosov Moscow State University, Vorob'evy gory, 119992 Moscow, Russia

Received 16 May 2002
Kvantovaya Elektronika **32** (9) 789 – 792 (2002)
Translated by J.M. Mikhailova

cells of two identical synchronously pumped dye lasers. The cavity of each of these lasers included an additional short (~ 2 mm) low-Q cavity, formed by inner window surfaces (with reflection coefficients of 0.1 % and 50 %) of a cell with the FN-70-dye. This configuration provided a fast seeding of picosecond lasing. By turning highly reflecting mirrors of spectral-selective 'synchronous' cavities of the dye lasers, whose lengths were matched with the MO-cavity length, the wavelengths $\lambda_{1,2}$ of laser radiation could be tuned within the range of 590 – 645 nm.

Lasing frequencies of both dye lasers were controlled with a spectrometer with the ~ 4 cm^{-1} resolution (1200 lines mm^{-1} grating working in the second order of diffraction was used). For absolute calibration of the wavelength λ_1 of radiation of one of the dye lasers, an interference filter with a passband less than 1 nm was used. To match the wavelength λ_2 of the second dye laser with λ_1 ($\lambda_1 = \lambda_2 = \lambda_p$), we tuned the cavity of that laser in such a way as to achieve the maximum self-diffraction efficiency η for the pulses of both dye lasers in a thin ($L \sim 10$ μm) GaSe film. The matching accuracy was determined by the lasing spectrum width $\delta\omega$ and was approximately equal to 1 cm^{-1}. The coarse and fine matching of cavity lengths involved achieving maximum energies of the dye-laser pulse train and its second harmonic (a 1-mm-long KDP crystal, oo – e interaction). Radiation from each dye laser represented a train of five pulses of virtually equal durations $\tau_p \sim 20$ ps with a peak power up to 50 kW for $\delta\omega \sim 1.5$ cm^{-1}. The parameters τ_p and $\delta\omega$ were measured by the correlation technique (noncollinear second-harmonic generation and self-diffraction in KDP and GaSe crystals were used). Dye laser beams were focused by lenses (focal length $f =$ 400 mm) and were directed to the tested sample at the angle $\Theta \sim 7^\circ$. The angle Θ determined the period $\Lambda = \lambda_p \times [2 \sin(\Theta/2)]^{-1}$ (about 5 μm for $\lambda_p = 620.4$ nm) of the spatial modulation of optical parameters of tested films in the interference field of two pump components. The timing of dye-laser pulses was achieved with the use of delay lines. The plane of the sample location and the values of f were chosen in such a way as to ensure the radiation resistance of tested films (the absence of irreversible changes).

The detection system used in our experiments had five independent input channels. The energies of pulses of the first and the second harmonics of the MO radiation, as well as the radiation energies of two dye lasers and the nonlinear signal were automatically monitored. As the nonlinear signal, self-diffraction pulses generated in the tested film were used. To detect the energy in control channels we used integrating photodiodes. The nonlinear signal was detected by a FEU-119 photodetector, working in a similar mode. The variance of the nonlinear signal was lowered by digital gating (programmable discriminator), which set limits from above and below for the maximum permissible values of signals in each of the control channels. Realisations where the level of at least one of the control signals missed the gate were discarded. With the gate width set equal to two standard deviations in each of the control signals, 50 % – 80 % of realisations satisfied the selection criteria.

Our detection system allowed us to detect the nonlinear signal in experiments with metal films with a thickness down to 10 nm. For the maximum (in best samples) signal-to-noise ratio ($\sim 10 - 30$), the dynamic range of measurements reached $\sim 10^2$, which provided a satisfactory reproducibility of the experimental results.

3. Tested samples

We investigated ultrathin metal Au and Pt films deposited on K8 glass substrates by laser evaporation at the Institute of Advanced Laser and Information Technologies, Russian Academy of Sciences. The method of mechanical and chemical polishing employed to prepare substrates provided a typical size of roughnesses of working surfaces less than 5 nm. Nevertheless, to choose the best substrates from the fabricated lot, the level of the dye-laser radiation scattering was measured before the deposition. The thickness L of deposited films was monitored both in the process of film production and after the completion of this process. The number of laser pulses used for this procedure (about 10 pulses were required to deposite a monolayer) was taken into account. The so-called four-point scheme was applied to measure the electric conductivity of the fabricated films. After the completion of this process, rough and precise estimates of L were made using the reflection and transmission coefficients and X-ray reflexometry data. Measurements of the electric conductivity for Au films with $L < 20$ nm revealed a cluster structure of these films. The results of experiments performed with the samples of that thickness noticeably varied when the film area exposed to the dye laser beam changed. Moreover, the cluster structure itself proved to change under laser beam exposure. Therefore, we describe below the reproducible results obtained for known-continuous samples of Au and Pt films 30 – 40-nm thick.

4. Experimental results

Wavelengths of both dye lasers in our experiments were simultaneously tuned ($\lambda_1 = \lambda_2 = \lambda_p$) within the range of 620.4 – 635.1 nm. At the same time, a series of measurements with a slight (± 10 cm^{-1}) variation in the frequency of one of the dye lasers was performed for each point (with a fixed value of λ_p). The frequency matching point ($\lambda_1 = \lambda_2$) was determined from the maximum of the self-diffraction efficiency η. Figs 1 and 2 show experimental dependences $\eta(\lambda_p)$ for continuous ultrathin Au and Pt films. These dependences represent the results of three series of experiments, with the dye-laser beam focused into different points on the sample. The coincidence of the results indicates that either the tested films were virtually homogeneous or the size of their inhomogeneities was much less than the size of the focal spot of the dye-laser beam (100 – 150 μm).

The most important experimental finding is that the dependences $\eta(\lambda_p)$ for Au and Pt films display a characteristic behaviour: the rise of η (at $\lambda_p \sim 622$ nm for Au and 629 nm for Pt) is followed by a dip at $\lambda_p \sim 632 - 635$ nm. Note that authors of similar experiments on the nonlinear spectroscopy of thin YBaCuO, Cu, C_{60}, and Ni films [9, 10, 17 – 19] already reported on a dip in the nonlinear response at the probing wavelength of ~ 632 nm. The importance of this fact is obvious. Indeed, if we assume that the self-diffraction signal is caused by spectrally nonselective processes related to absorption by free carriers and the subsequent writing of acoustic and/or thermal diffraction gratings [13] in a sample, then η should not depend on λ_p.

Thus, the nonmonotonic behaviour of the dependences $\eta(\lambda_p)$ for Au and Pt films (Figs 1, 2) indicates the importance of interband transitions in the formation of the

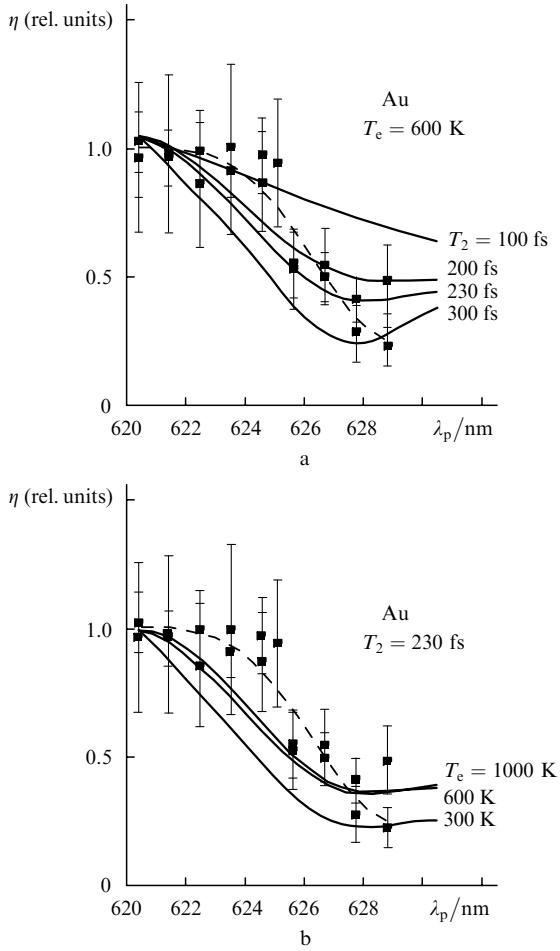

Figure 1. Experimental data (dots), their polynomial fit (dashed curves), and calculated dependences $\eta(\lambda_p)$ (solid curves) for an Au film at $T_e = 600$ K with different T_2 (a) and $T_2 = 230$ fs with different T_e (b); $L = 5$ nm, $S = 0.01$.

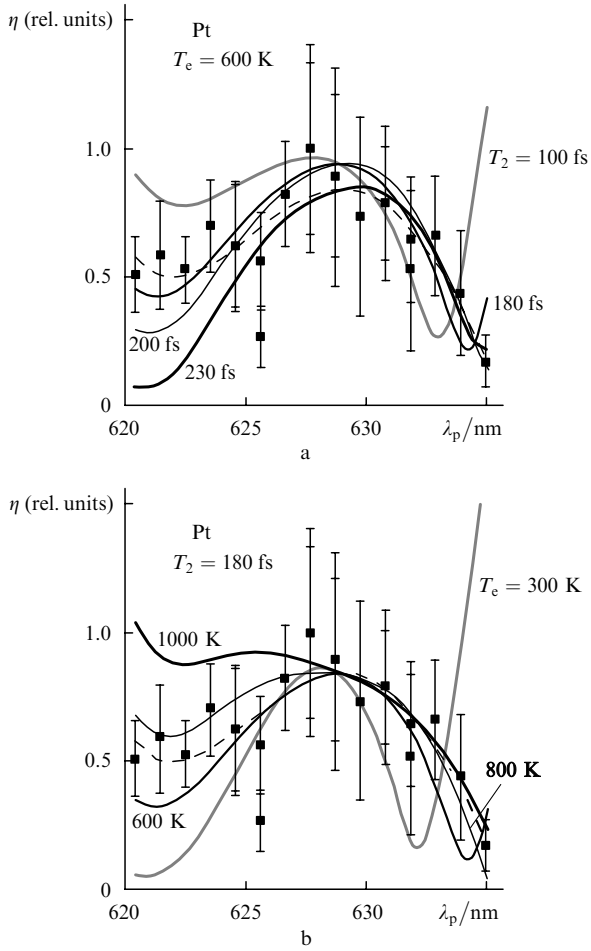

Figure 2. Experimental data (dots), their polynomial fit (dashed curves), and calculated dependences $\eta(\lambda_p)$ (solid curves) for a Pt film at $T_e = 600$ K with different T_2 (a) and $T_2 = 180$ fs with different T_e (b); $L = 5$ nm, $S = 0.01$.

coherent nonlinear response of metal films in the optical range. Indeed, within the framework of this assumption, if we take into account the sufficiently high (~ 2 eV) energy of the pump photon, the excitation process should influence the carrier distribution in several energy bands. In this case, the superposition ('interference') of contributions from several simultaneous interband transitions may lead to the spectral selectivity of the coherent nonlinear response.

5. Numerical simulation

Experimental results were interpreted in terms of the electronic nonlinear susceptibility model, which takes into account the saturation of interband electron transitions in the spectrum of electronic states of ultrathin metal films [9]. The data for the interpolation of the energy-band structure of Au and Pt onto the entire Brillouin zone were borrowed from [20, 21]. Computational results were fitted to the experimental data with the following free parameters: the effective temperature T_e of the electron subsystem, the unified relaxation parameter T_2, and the maximum level S of the relative variation in the population of electronic states. The temperature T_e was changed from 1000 to 300 K (estimates of T_e in the case of a slow and fast energy removal from the electron subsystem), which covered the range of T_e estimates (600 – 800 K) obtained by different authors [2, 19, 22] for similar excitation regimes. The parameter T_2 was considered to be a result of the combined effect of all intra- and interband relaxation processes and was varied from 50 to 700 fs. The value of S was varied from 1 % to 10 %, because for the used excitation levels ($10^{-3} - 10^{-4}$ J cm^{-2}) and comparatively long pump pulses ($\tau_p \sim 20$ ps), it was unlikely that occupation numbers could change substantially.

Note that the calculation performed in [23] for the narrow-gap semiconductor PbTe showed that the value of S mainly influenced the nonlinear response amplitude. However, in metal films, where the Fermi level E_F crosses one or even several energy bands, saturation may be much more important, since electron states separated by large energy intervals from the Fermi level E_F start to play a more noticeable role.

The spectroscopic information was obtained from the experimental data in the following way. Series of dependences $\eta(\lambda_p)$ were calculated for different values of T_e, T_2, and S. A set of parameters was considered as reasonable in the cases when the dependences had the same specific features as the experimental dependences. The results of calculation of $\eta(\lambda_p)$ for Au and Pt films presented in Figs 1, 2 by solid curves (similar results have been reported

for Ni films [9]) strongly depend on the T_2 value. Results of calculation for Au films satisfactorily (within error limits, Fig. 1a) agree with the experimental data for $T_2 = 230\pm$ 30 fs, which is consistent with the results of [1]. Variations in T_e and S almost do not change the character of $\eta(\lambda_p)$ (Fig. 1b). The results of calculations for Pt films correspond to the experimental data for $T_2 = 180 \pm 30$ fs (Fig. 2a). In this case, variations in T_e have a much stronger influence on the character of $\eta(\lambda_p)$ (Fig. 2b), which allows one to estimate possible values of this parameter as well: $T_e = 600 - 800$ K.

6. Conclusions

Thus, our calculations have shown that the specific features of substantially nonmonotonic experimental dependences $\eta(\lambda_p)$ can be reproduced with an appropriate choice of only two free parameters (T_2 and T_e) of the model, which takes into account the coherent superposition of contributions from a large number of saturable interband electronic transitions. Therefore, we can argue that, for a sufficiently high photon energy (comparable with or exceeding 2 eV), the four-photon response of ultrathin metal films to picosecond excitation is mainly due to this mechanism of nonlinearity. Because of the interference of contributions of several interband transitions, the nonlinear response in the DFWM method is extremely sensitive to variations in the phases of separate components, depending on characteristic times of intraband relaxation processes. This fact allows one to estimate these times quite precisely ($\pm 10\,\%$). As mentioned above, today we know three groups of authors [10–12], who came out with an idea of a paramount role of interband electronic transitions in the processes involving the formation of the nonlinear response of metal films to pico- and femtosecond optical pulses.

Acknowledgements. This work was supported by the Russian Foundation for Basic Research (Grant No. 02-02-16603) and FTsNTP 'Investigations and Developments in Priority Directions of Science and Technology Progress'.

References

1. Vaterlaus A., et al. *Phys. Rev. Lett.*, **67**, 3314 (1991).
2. Fann W.S., et al. *Phys. Rev. B*, **46**, 13592 (1992).
3. Wright O.B. *Phys. Rev. B*, **49**, 9985 (1994).
4. Hohlfeld J., et al. *Phys. Rev. Lett.*, **78**, 4861 (1997).
5. Hohlfeld J., et al. *Appl. Phys. B*, **68**, 505 (1999).
6. Hohlfeld J., et al. *Chem. Phys.*, **251**, 237 (2000).
7. Akhmanov S.A., Koroteev N.I. *Metody nelineinoi optiki v spektroskopii rasseyaniya sveta* (Methods of Nonlinear Optics in Light Scattering Spectroscopy) (Moscow: Nauka, 1981).
8. Petnikova V.M. et al. *Kvantovaya Elektron.*, **28**, 69 (1999) [*Quantum Electron.*, **29**, 626 (1999)].
9. Kuznetsova L.P., et al. *Kvantovaya Elektron.*, **30**, 175 (2000) [*Quantum Electron.*, **30**, 175 (2000).]
10. Lozovik Yu.E., et al. *Phys. Lett. A*, **223**, 303 (1996).
11. Pawlik S., et al. *Surface Science*, **377–379**, 206 (1997).
12. Aeschlimann M., et. al. *J. of Electron Spectroscopy and Related Phenomena*, **88–91**, 179 (1998).
13. Gusev V.E., Wright O.B. *Phys. Rev. B*, **57**, 2878 (1998).
14. Gantmacher V.F., Levinson I.B. *Rasseyaniye nositelei toka v metallakh i poluprovodnikakh* (Current Carrier Scattering in Metals and Semiconductors) (Moscow: Nauka, 1984).
15. Alig R.C. *Phys. Rev.*, **178**, 1050 (1969).
16. Ustinov V.V., Okulov V.I. *Fiz. Met. Metalloved.*, **37**, 39 (1974); **37**, 263 (1974).
17. Bobyrev Yu.V., et al. *Kvantovaya Elektron.*, **31**, 1067 (2001) [*Quantum Electron*, **31**, 1067 (2001)].
18. Farztdinov V.M., et al. *Phys. Rev.*, **56**, 4176 (1997).
19. Dobryakov A.L., et al. *Phys. Scripta*, **60**, 572 (1999).
20. Seraphin B.O., Cristersen N. *Phys. Rev. B*, **4**, 3321 (1971).
21. Friedel J., et al. *Chem. Sol.*, **25**, 781 (1964).
22. Sun C.-K., et al. *Phys. Rev B*, **50**, 15337 (1992).
23. Vereschyagina L.N., et al. *Zh. Eksp. Teor. Fiz.*, **109**, 923 (1996) [*JETP*, **109**, 923 (1996)].